

Assessment of a Finite Element Geothermal Reservoir Simulator on Benchmark Problems

FALCON Code Verification & Validation and New Feature Development

Yidong Xia, Hai Huang, and Robert Podgorney

Department of Energy Resource Recovery & Sustainability
Energy and Environment Science & Technology Directorate
Idaho National Laboratory

yidong.xia@inl.gov



Presented at

2015 International Conference on Coupled Thermo-Hydro-Mechanical-Chemical (THMC) Processes in Geosystems

Salt Lake City, Utah, USA

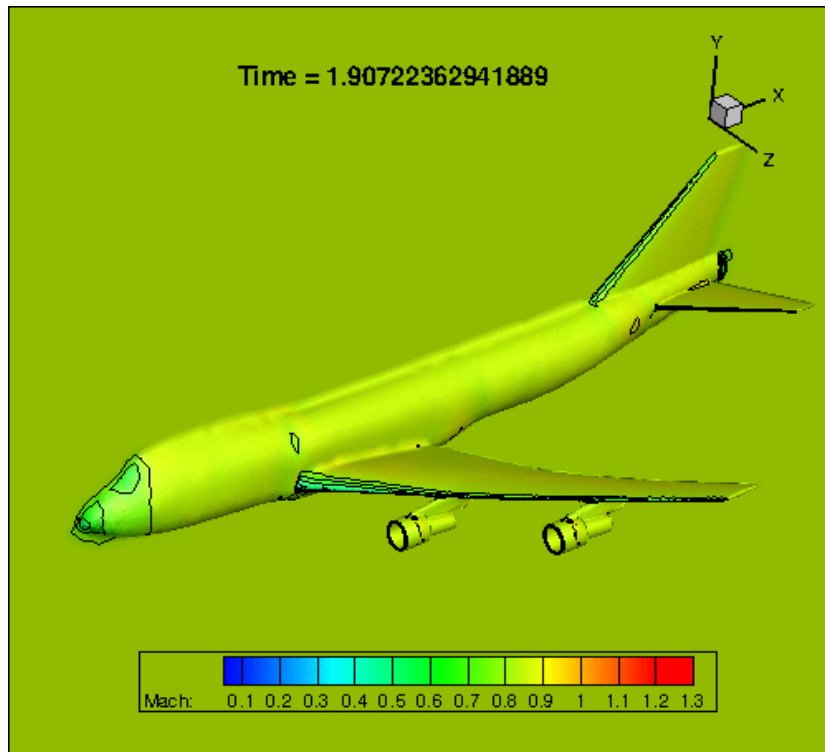
February 25 – 27, 2015

www.inl.gov

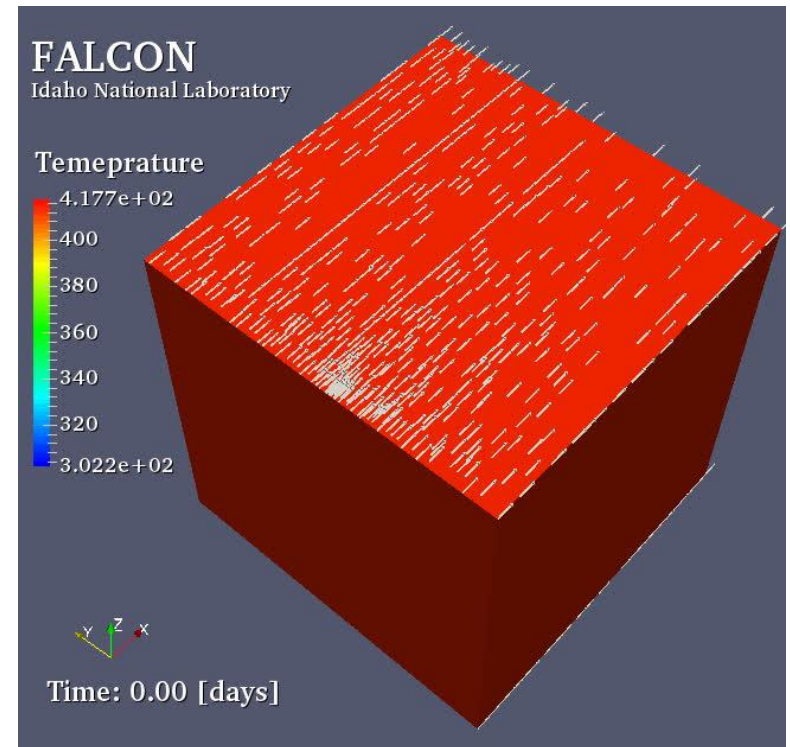


Who Am I?

--- Past ---



--- Now ---



Outline and Acknowledgment

- Outline
 - Objective of this work
 - Introduction to the **FALCON** code
 - **New** features currently under development
 - A few geothermal, geomechanical examples & benchmark problems
- Acknowledgment
 - **INL**: Derek Gaston, Cody Permann, Mitch Plummer
 - **U. of Utah**: Luanjing Guo, Jacob Bradford, Raili Taylor, Surya Sunkavalli
 - **Others**: CSIRO, U. of Western Au., U. of NSW, U. of Auckland

Code Verification and Validation (V&V)

- **FALCON** code
 - Stands for Fracturing And Liquid CONvection
 - Built based on INL's **MOOSE** framework <http://www.mooseframework.com/>
 - Physics-based, massively parallel, fully-coupled, **finite element** model for simultaneously solving multiphase fluid Flow, heat transport, and rock deformation for geothermal reservoir simulation
- Why **V&V**
 - Any code must undergo an extensive and rigorous V&V process, before they can be trusted and used for solving problems of practical importance.
 - V&V testing is an essential part of the software quality control, which is especially crucial for the development of the FALCON code.

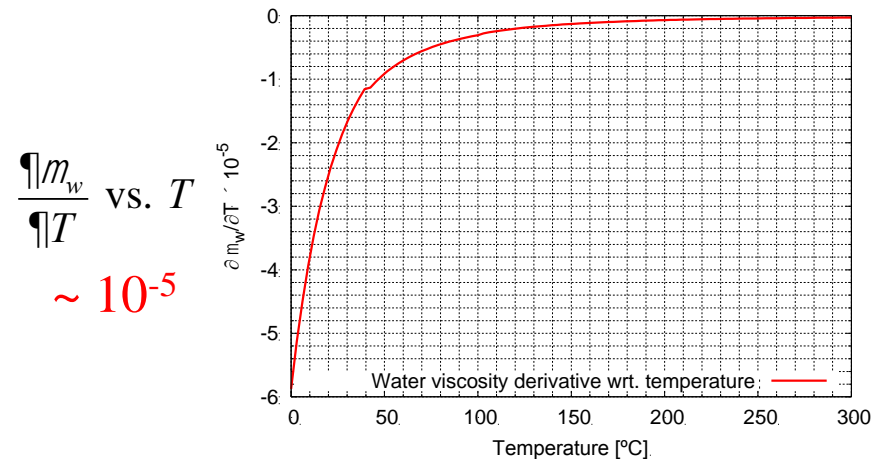
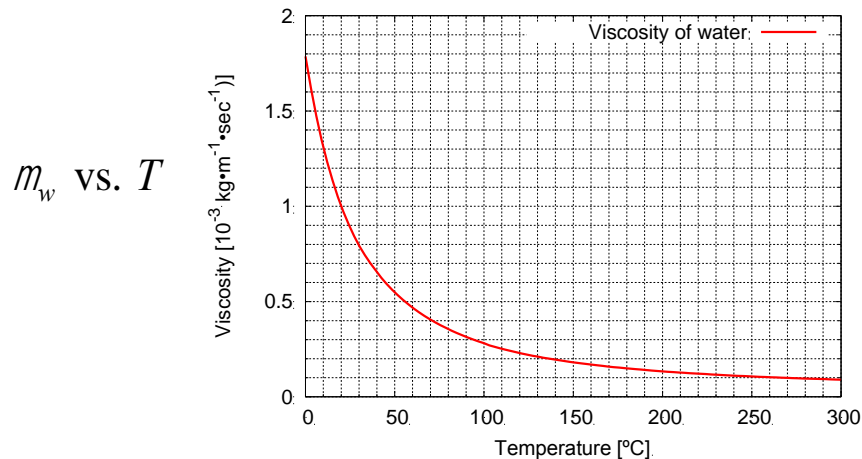
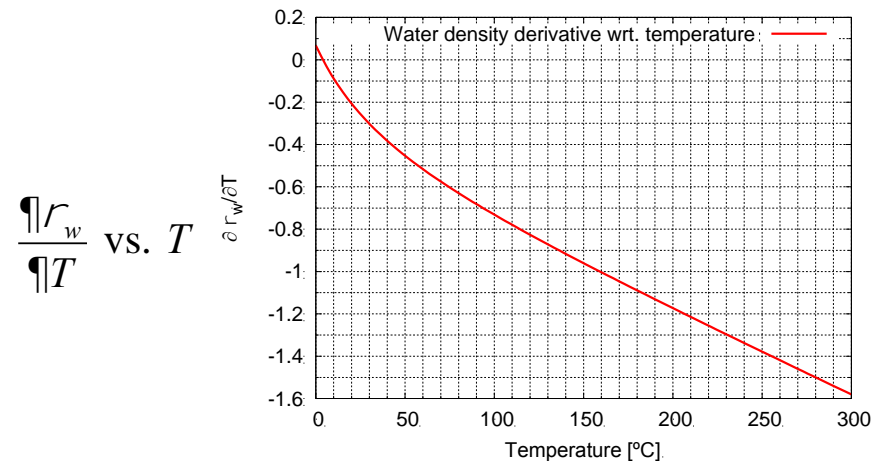
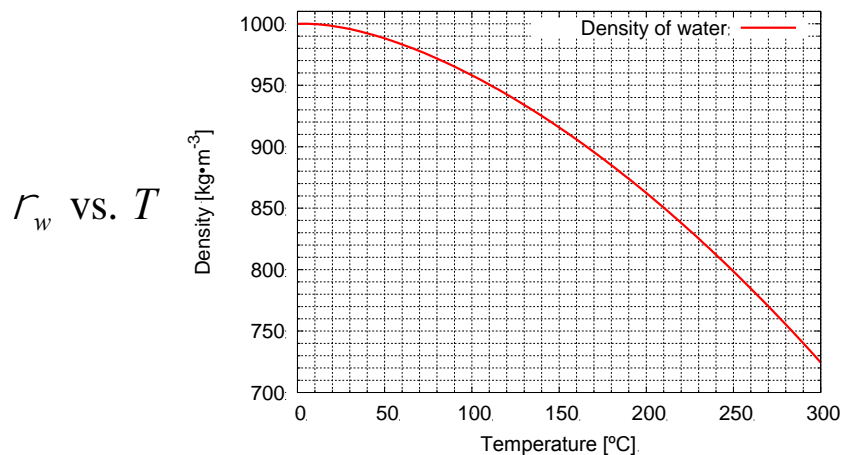
Coupled THM in Porous Media

- Scope of the present work
 - Pressure-temperature-displacement based formulation for single-phase flow of water in a deformable, compressible geologic medium

$$\left\{ \begin{array}{l}
 \frac{\partial(fr_w)}{\partial t} - \nabla \cdot \left[\frac{kr_w}{m_w} (\nabla p_w + r_w g \nabla z) \right] - q'_w = 0 \\
 [fr_w c_w + (1-f)r_r c_r] \frac{\partial T}{\partial t} - \nabla \cdot (K_m \nabla T) + r_w c_w \mathbf{q} \cdot \nabla T = 0 \\
 r \frac{\partial^2 \mathbf{u}}{\partial t^2} - \nabla \cdot \mathbf{S} + r g \nabla z - a \nabla p - b K \nabla T = 0
 \end{array} \right.$$

Constitutive Relationships

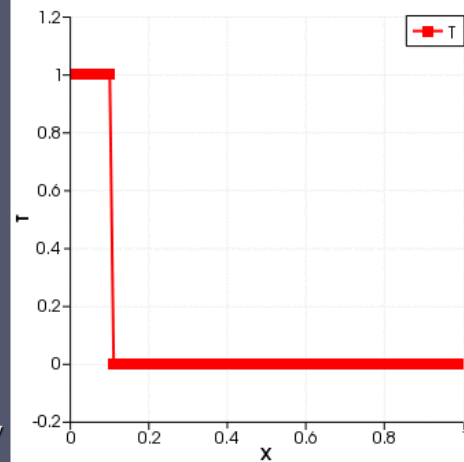
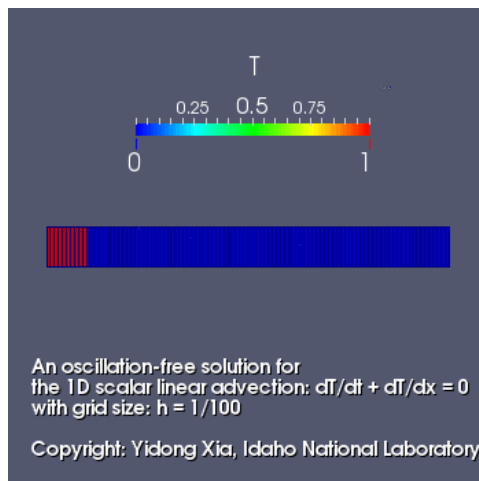
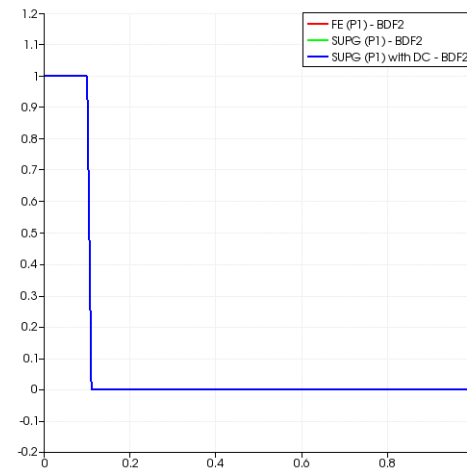
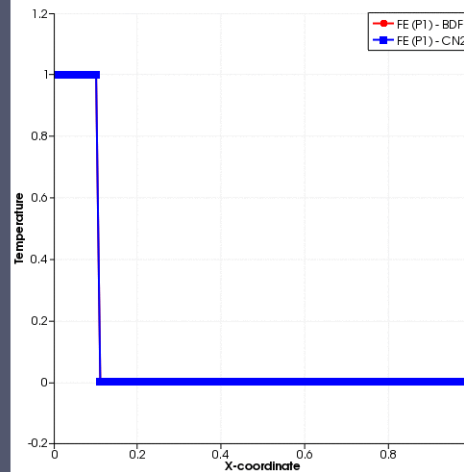
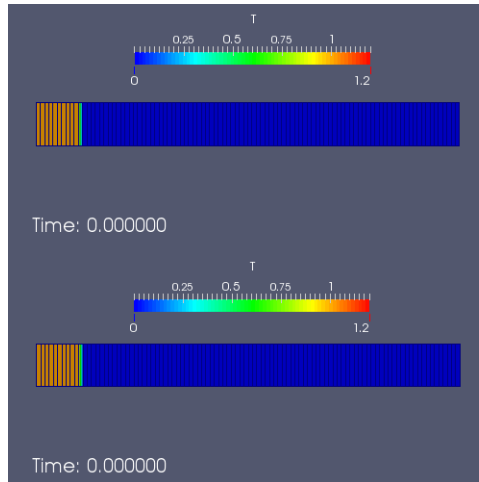
- Two options
 - 1) Analytical functions $\rho_w = f(T)$, $\mu_w = g(T)$ for $T = [0, 300]^\circ \text{C}$



Constitutive Relationships

- Two options
 - 2) Water-steam EOS based on IAPS-97 formulation
 - Covers a wider range, e.g., water, steam, and water-steam situations
 - Derivatives computed by **Divided-Difference (DD)**
 - ☐ Easy to implement
 - ☐ Slow, less accurate and could result in instability for highly nonlinear problems
 - Derivatives computed through **Automatic-Differentiation (AD)** codes. **new!**
 - ☐ Fast – properties and their derivatives calculated at the same time
 - ☐ Accurate, robust for highly complicated formulations
 - ☐ Need developer's understanding of AD on some degree

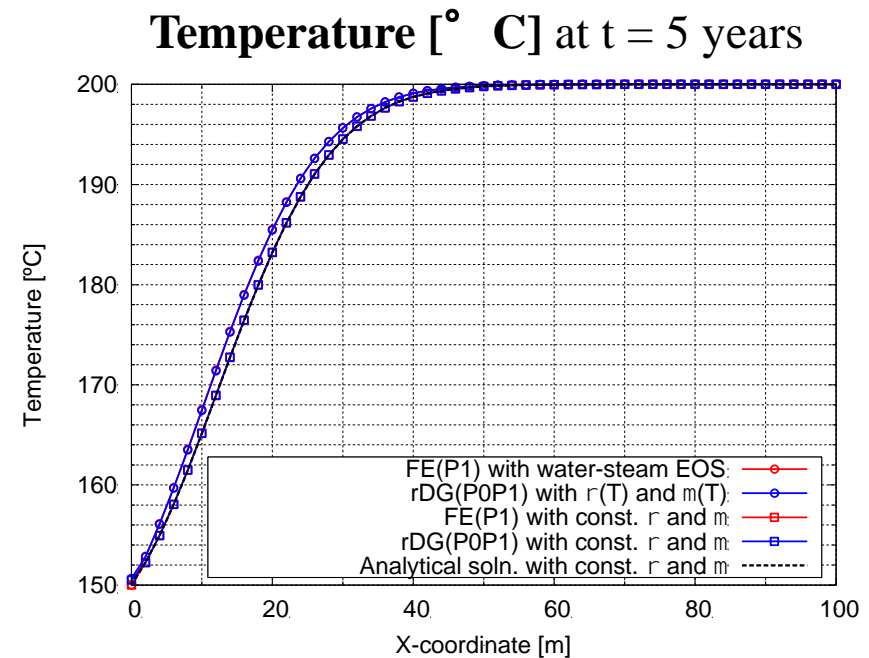
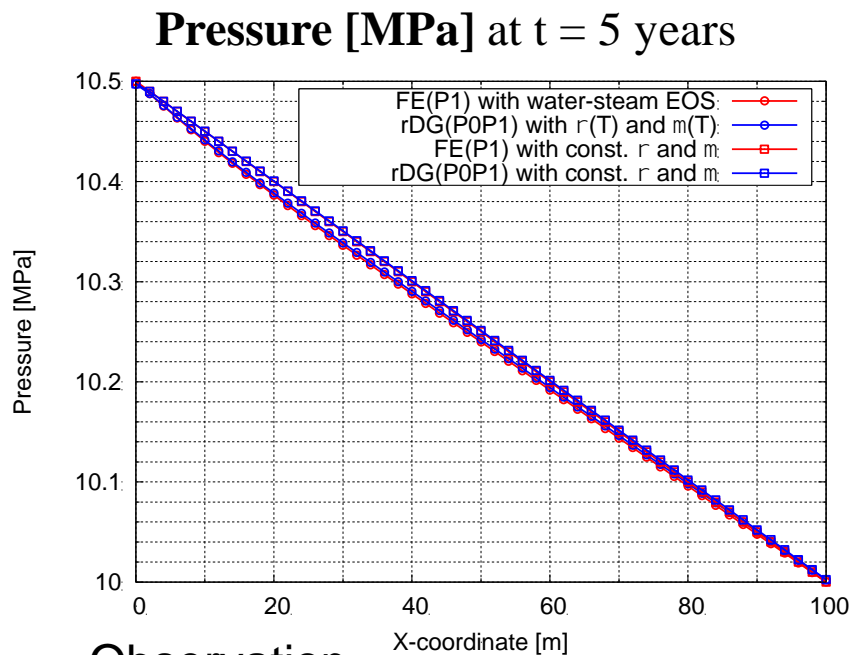
Non-physical oscillations near Thermal Fronts



reconstructed discontinuous Galerkin methods – rDG, *new!*
that combine the advantages of both **Finite Element** and **Finite Volume** methods

Case 1. Comparison to 1D Analytical Solution

- An 1D heat conduction-convection solution, see **Faust & Mercer, 1979**
 - Omit the heat exchange between confined aquifer and surrounding rock
 - Constant water density ρ_w and viscosity μ_w

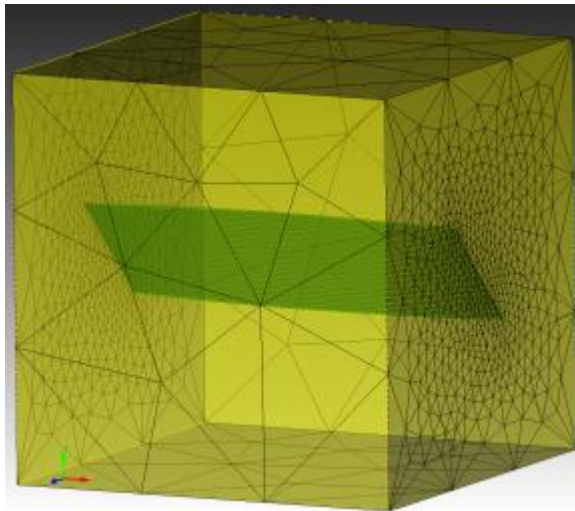


Observation

- rDG matches well to FE
- T -dependent functions for ρ_w and μ_w match well with water-steam EOS

Case 2. Cold Water Injection in Hot Fractured Zone

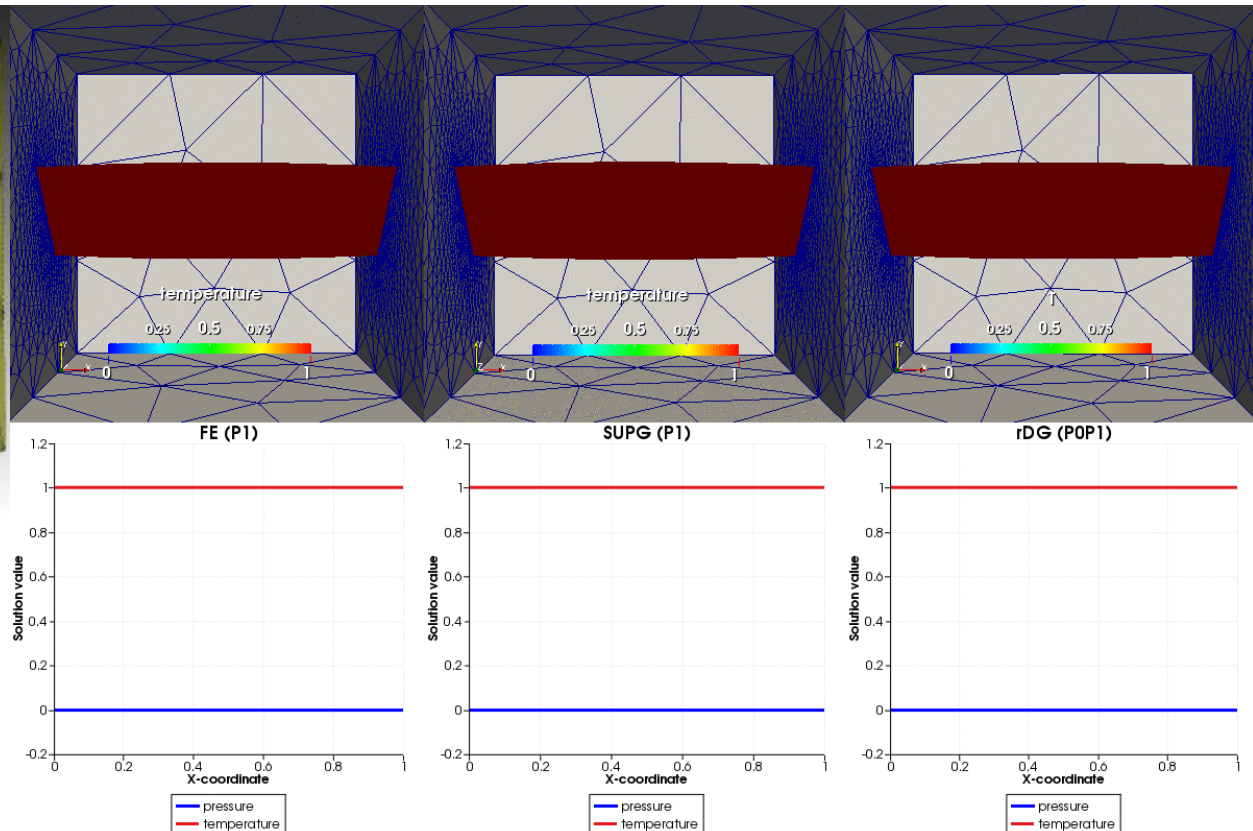
- Injection of cold water through a hot fractured rock zone
 - Peclet number = 1000 (strongly convective)



Computational mesh

$(x, y, z) =$
 $([-0.5, 0.5], [-0.5, 0.5], [-0.5, 0.5])$

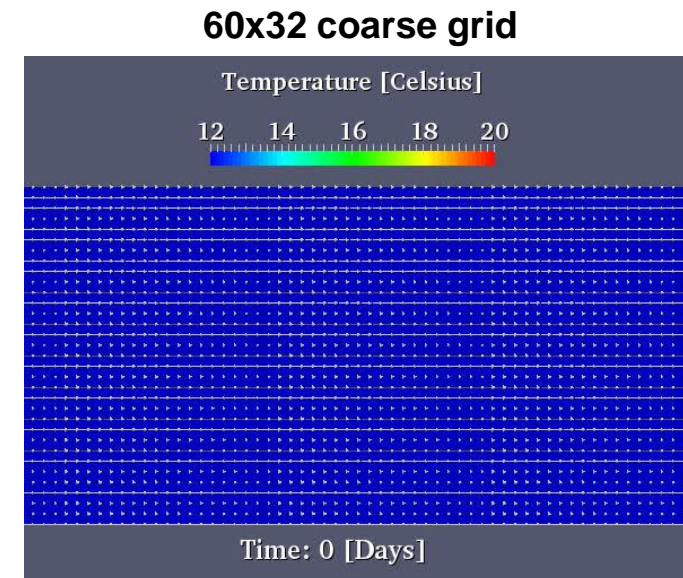
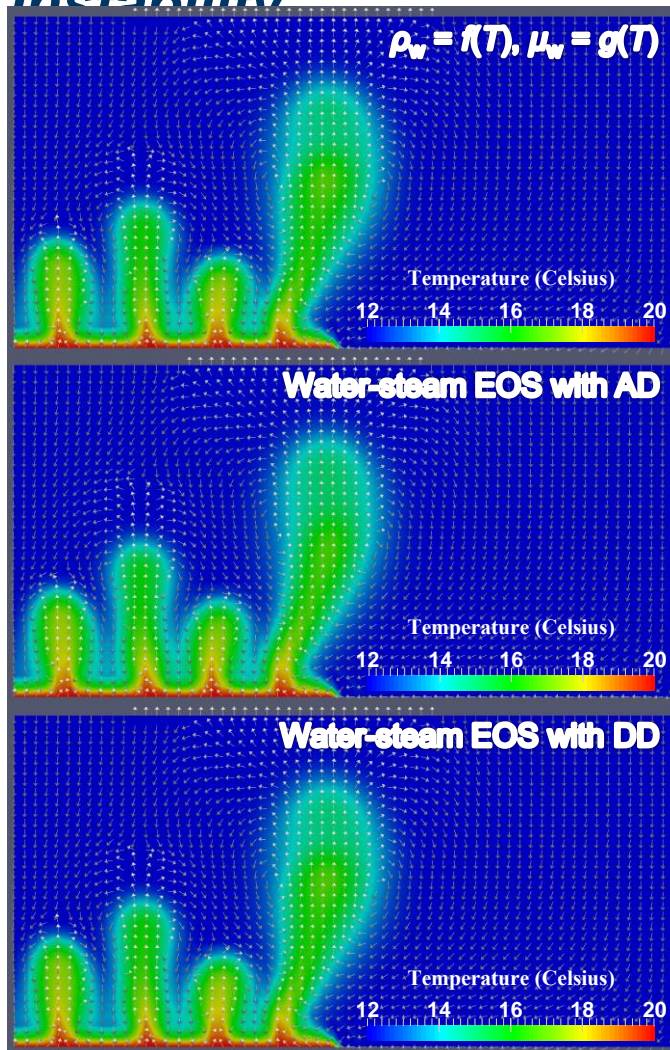
Hybrid elements



Case 3. Thermally Induced Buoyant Convection and Instability

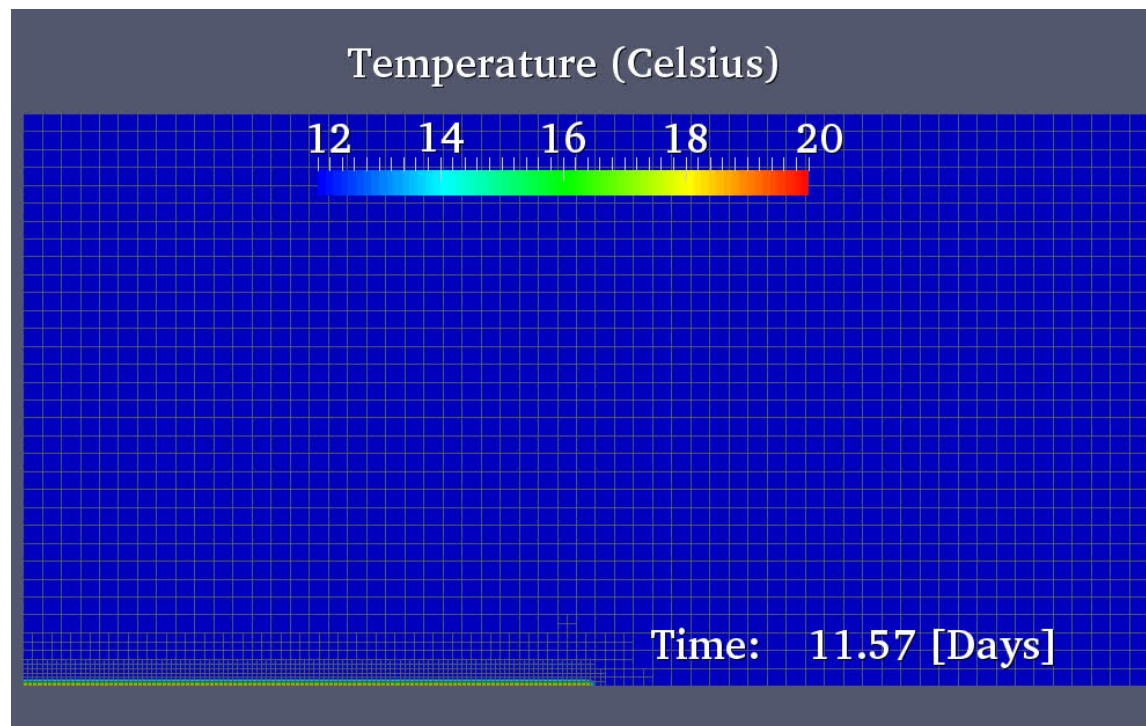
Initially introduced by **Elder in 1967**

- ☐ ρ_w -driven thermal convection in porous media due to non-uniform heating of a 2-D from bottom.
- ☐ Upwelling of warm water & formation of thermal fingering



Case 3. Thermally Induced Buoyant Convection and Instability

- Automatic Mesh Refinement (AMR) on the 60x32 coarse grid



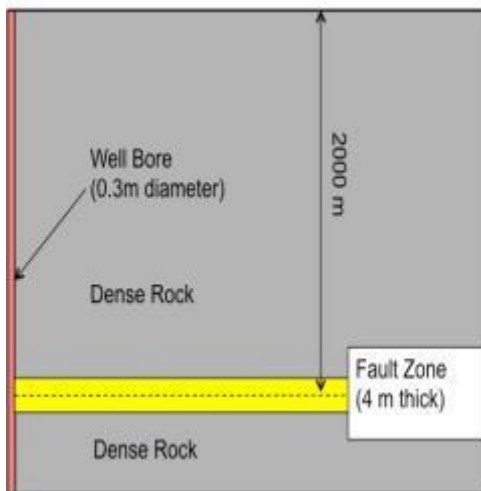
***h*-adaptivity vs. *p*-adaptivity?**

Case 4. Poroelastic/Thermal Transport in a Single Fracture

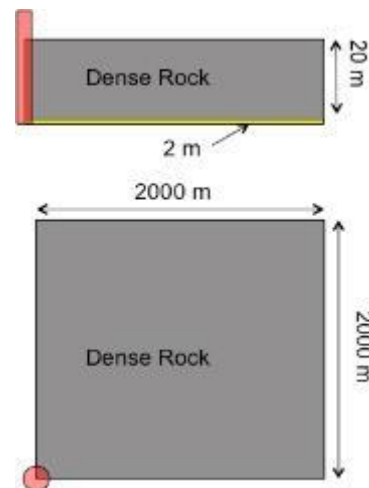
- Problem 1 in the [GTO Code Comparison Study](#)
 - Proposed by [H. Huang](#), [M. Plummer](#), and [R. Podgorney](#) at INL
- Source
 - Simplified resembling of the experimental site at the Raft River EGS demonstration in southern Idaho
- Why
 - Require only basic functionality for realistic geothermal simulation
 - Expect different codes (1D, 2D and 3D) to produce similar predictions
- Objective
 - Verify the fundamental thermal-hydraulic formulations in the codes
 - Serve as the basis for further challenging test cases

Case 4. Poroelastic/Thermal Transport in a Single Fracture

- Description of problem set-up
 - Poroelastic response (and later thermoelastic) to water injection into a geothermal reservoir



Cartesian
(1/8 model)



Radial

Boundary Conditions:

- ☐ Fixed injection rate at left wellbore
- ☐ Const. pressure and temperature at the vertical outer bound
- ☐ No-flow, zero-heat flux at symmetry and top bound

Boundary Conditions:

- ☐ Fixed injection rate at center
- ☐ Const. pressure and temperature at the outer bound

- ☐ Simulation time = 3 days
- ☐ Injection rate = 80 kg/s
- ☐ Initial pressure = 20 MPa
- ☐ Initial temperature = 140° C

☐ **Permeability for fault zone:** $k = k_0 \exp\left(\frac{c}{S} (p - p_0)\right)$

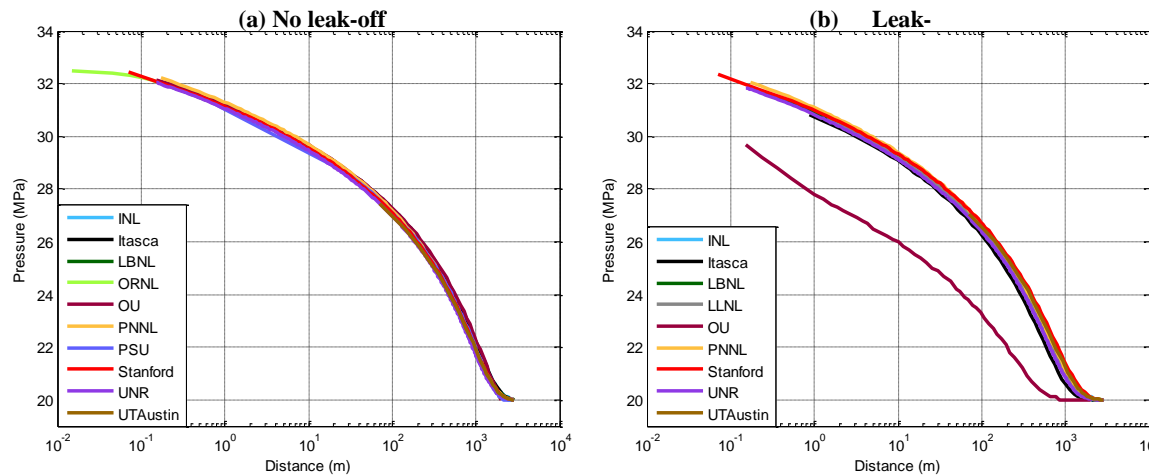
Case 4. Poroelastic/Thermal Transport in a Single Fracture

- Details of the 11 participating teams

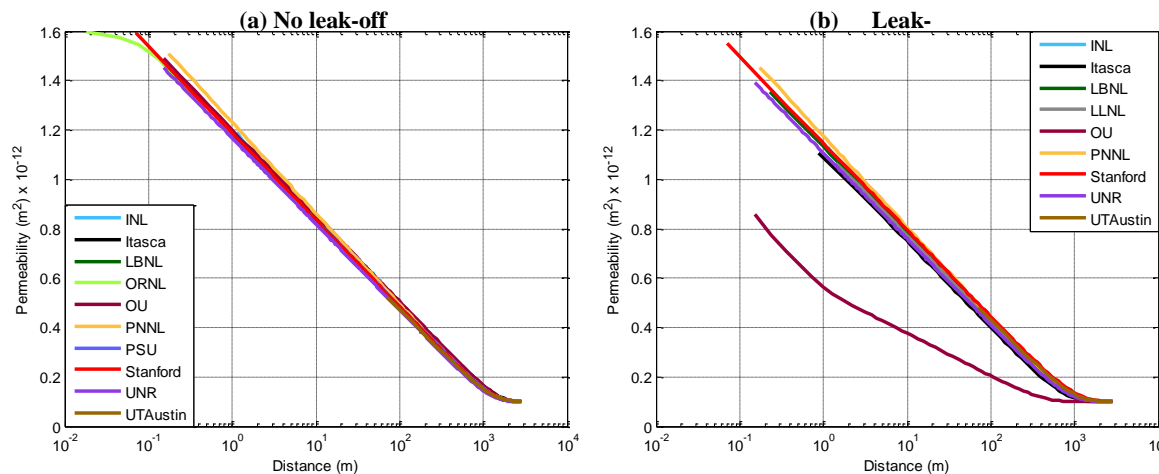
Teams	Codes	Methods	Topology & Mesh	Water density & viscosity
INL	FALCON	FEM	Unstructured Hex	water-steam EOS (based on IAPWS-1997)
Itasca	FLAC	FDM	2D Radial Quad	$\rho_w = \text{const}; \mu_w = \text{const}$
LBNL	TOUGH-FLAC	FDM	3D Radial Hex	1967 ASME steam table
LLNL	GEOS	FEM	Unstructured Hex	$\rho_w = \rho_{\text{ref}} \exp[c_w(p - p_{\text{ref}})]; \mu_w = \text{const}$
ORNL	PFLOTRAN	FVM		
OU		FEM	Unstructured Hex	$\rho_w = \text{const}; \mu_w = \text{const}$
PNNL	STOMP	FVM	1D for no-leakoff 2D radial for leakoff	1967 ASME steam table
PSU	TOUGH2-FLAC	FDM	2D Radial Quad	1967 ASME steam table
Stanford	CFRAC (Stanford)	FDM	3D Cartesian Hex	$\rho_w = \rho_{\text{ref}} \exp[c_w(p - p_{\text{ref}})]; \mu_w = \text{const}$
UN Reno	MULTIFLUX	FDM	2D Radial Quad	Variable viscosity and density
UN Austin	CFRAC (UT)	FVM	1D for fault zone Tria for rock zone	$\rho_w = \rho_{\text{ref}} \exp[c_w(p - p_{\text{ref}})]; \mu_w = \text{const}$

Case 4. Poroelastic/Thermal Transport in a Single Fracture

- Distribution of **pressure** along $[x = y, z = 2000]$ or $[r = 0.15 - 2828.4, z = 2000]$ at time = 10^4 sec



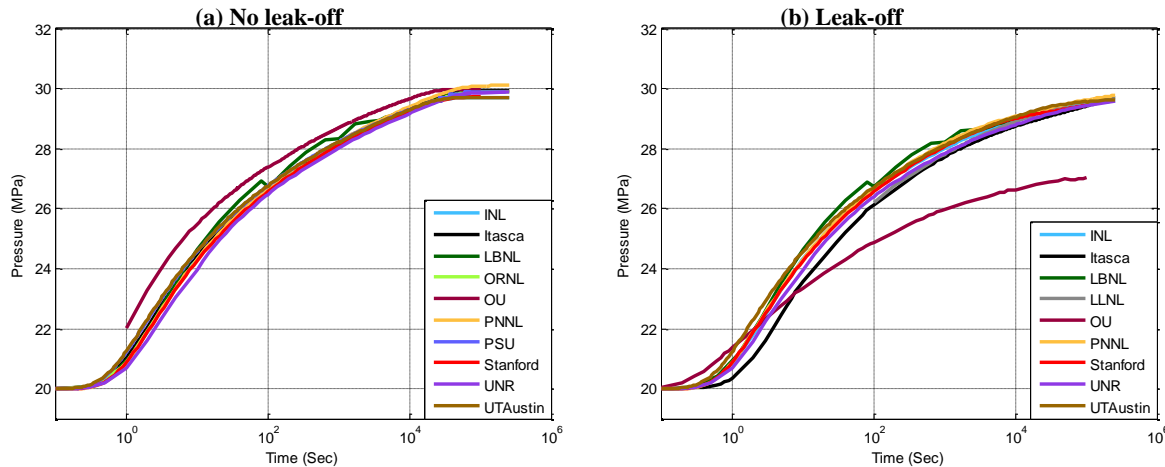
- Distribution of **permeability** along $[x = y, z = 2000]$ or $[r = 0.15 - 2828.4, z = 2000]$ at time = 10^4 sec



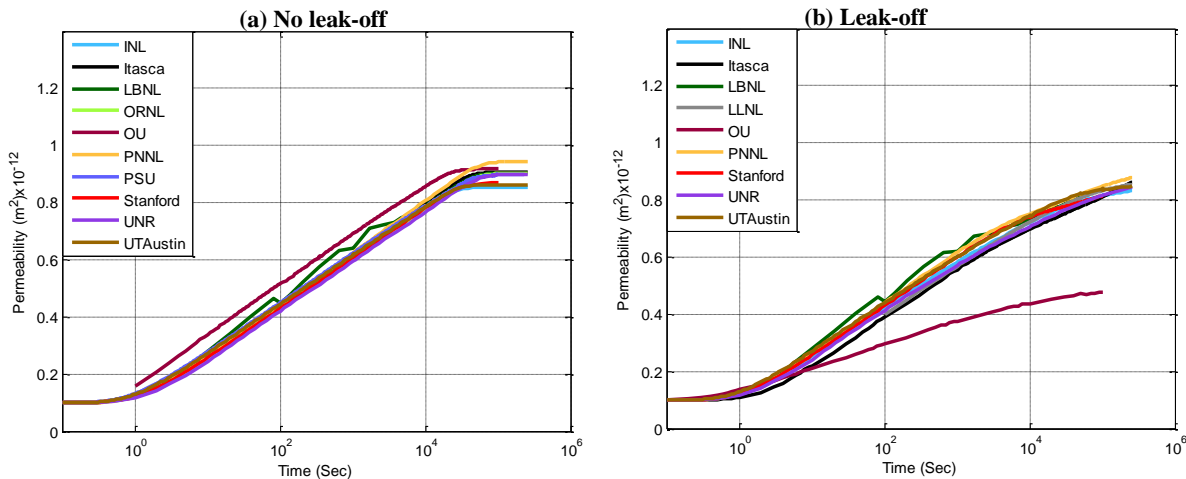
Artworks by
**D. Bahrami &
G. Danko** at
University of
Nevada,
Reno

Case 4. Poroelastic/Thermal Transport in a Single Fracture

- Time history of **pressure** at $(x, y, z) = (10, 10, 2000)$ or $r = 14.142$



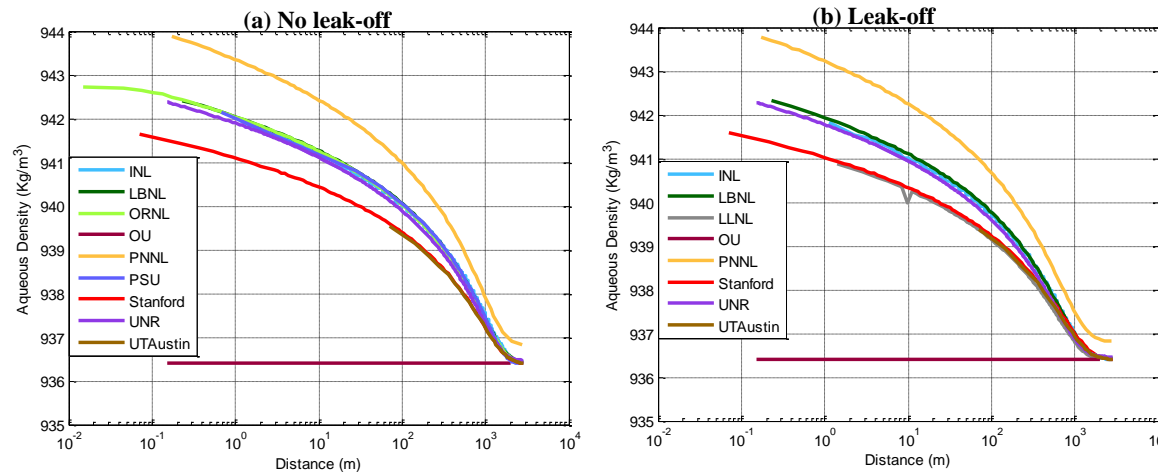
- Time history of **permeability** at $(x, y, z) = (10, 10, 2000)$ or $r = 14.142$



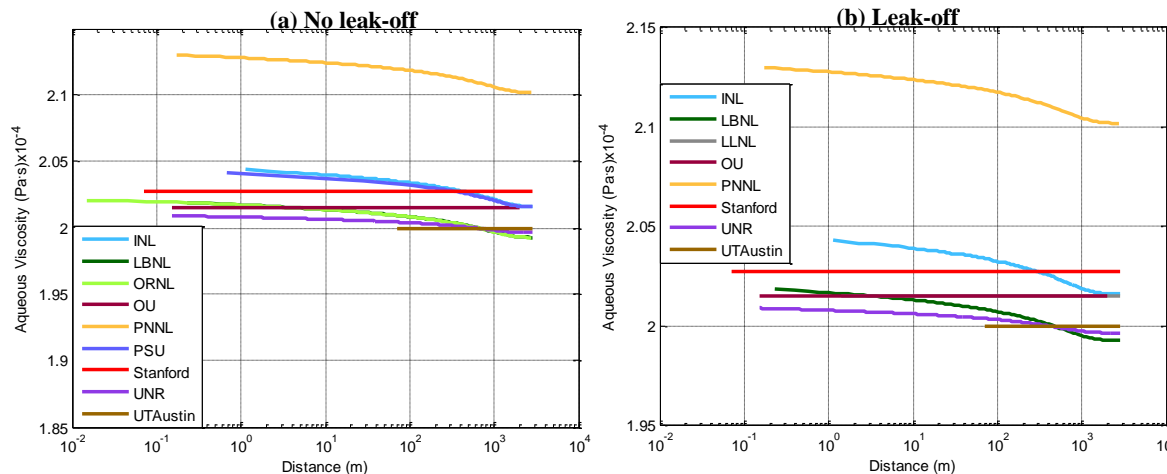
Artworks by
**D. Bahrami &
G. Danko** at
University of
Nevada,
Reno

Case 4. Poroelastic/Thermal Transport in a Single Fracture

- Distribution of **water density** along $[x = y, z = 2000]$ or $[r = 0.15 - 2828.4, z = 2000]$ at time = 10^4 sec



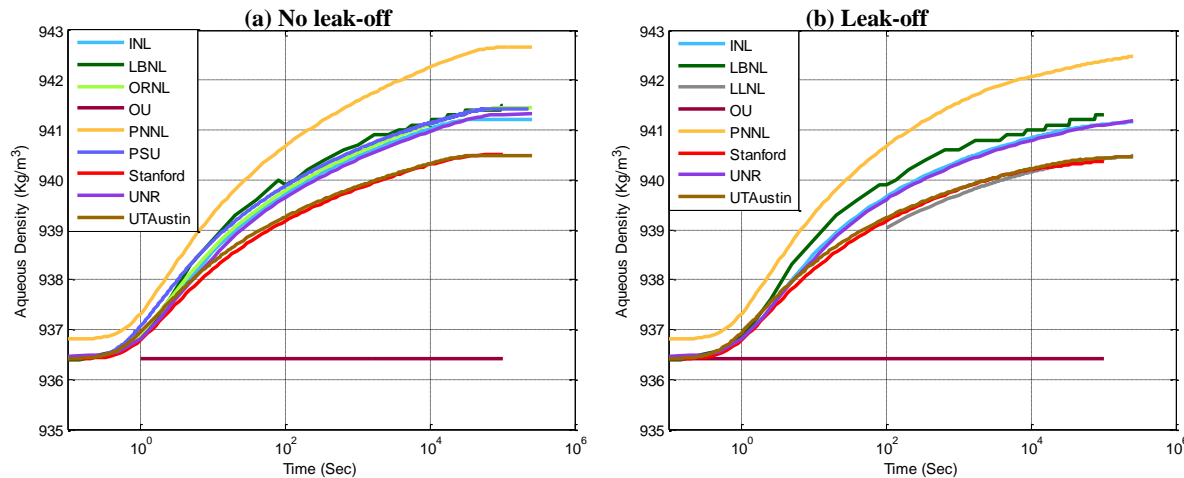
- Distribution of **water viscosity** along $[x = y, z = 2000]$ or $[r = 0.15 - 2828.4, z = 2000]$ at time = 10^4 sec



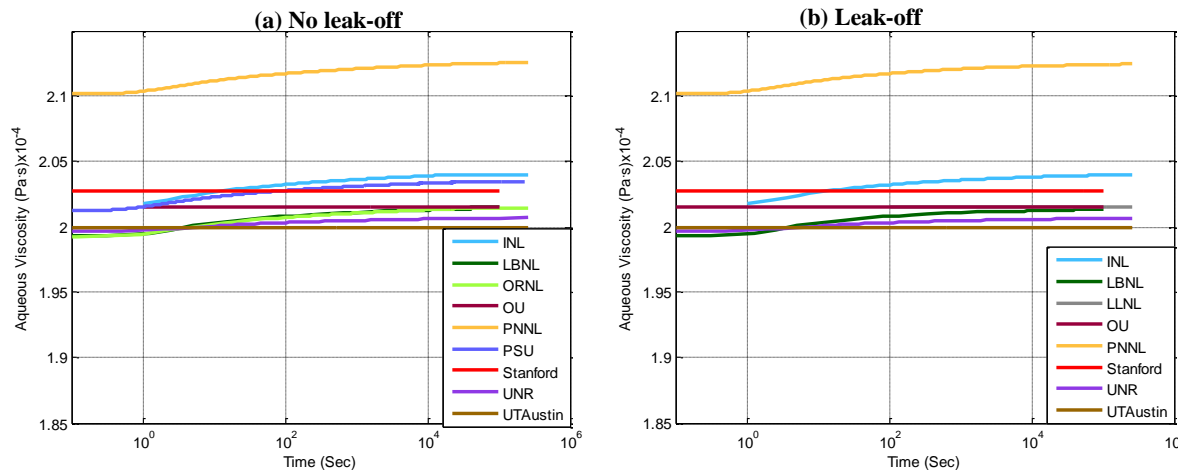
Artworks by
**D. Bahrami &
G. Danko** at
University of
Nevada,
Reno

Case 4. Poroelastic/Thermal Transport in a Single Fracture

- Time history of **water density** at $(x, y, z) = (10, 10, 2000)$ or $r = 14.142$



- Time history of **water viscosity** at $(x, y, z) = (10, 10, 2000)$ or $r = 14.142$



Artworks by
**D. Bahrami &
G. Danko** at
University of
Nevada,
Reno

Case 4. Poroelastic/Thermal Transport in a Single Fracture

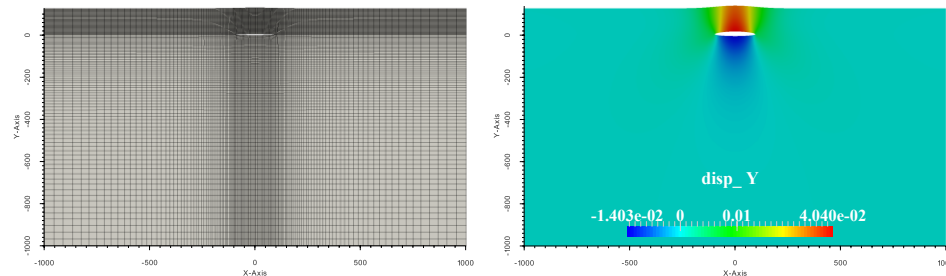
- Various model assumptions and successes have been shown for the solutions to GTO Code Comparison Study Problem 1.
- This case has served as an important first test problem for the validation of reservoir simulation codes against each other.
- The **assumption** of the given poroelastic characteristics of Natenson was followed in all models including the self-propped, open-fracture approach.
- The codes by all eleven teams delivered qualitatively close, comparable results.

Case 5. Quantifying Ground Surface Deformation

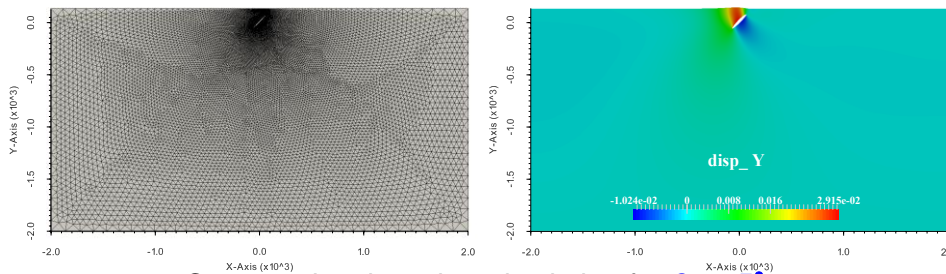
- Problem 7 in the **GTO Code Comparison Study**
 - Proposed by **P. Fu & B. Guo** at **Lawrence Livermore National Laboratory**
 - Based on a literature survey, the problem is designed loosely based on the plane-strain solution of Pollard & Holzhausen (1979).
- Why
 - Quantifying ground surface deformation caused by the hydraulic stimulation of subsurface reservoir is an important means for understanding reservoir characteristics and reservoir behavior.
 - For reservoirs dominated by discrete fractures and stimulations that create discrete fractures, surface deformation measurements can be particularly useful in identifying the stimulated fractures and estimating their dimensions.
- Objective
 - Compare the ability to predict ground surface deformations caused by the pressurization of a subsurface fracture of various codes currently used for geothermal reservoir modeling.

Case 5. Quantifying Ground Surface Deformation

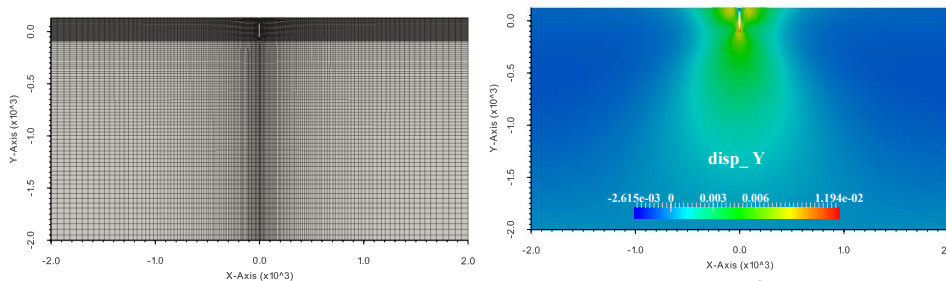
- Contours of vertical displacement (deformation is exaggerated for display purpose)



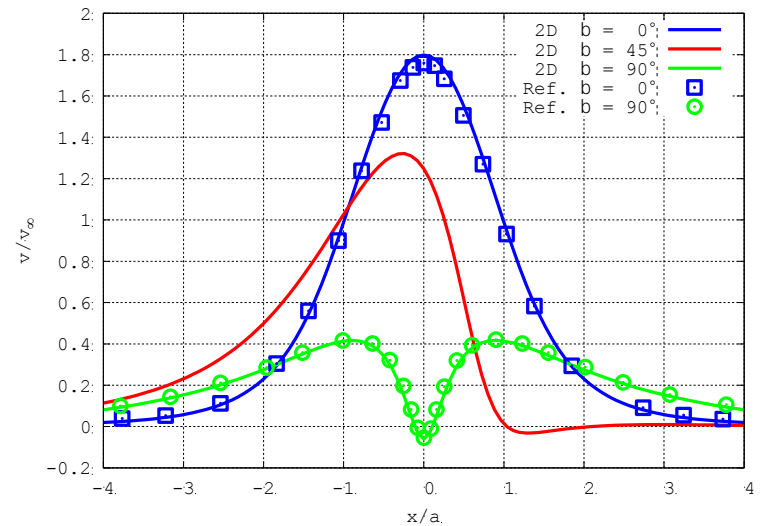
Computational mesh and solution for $\beta = 0^\circ$



Computational mesh and solution for $\beta = 45^\circ$



Computational mesh and solution for $\beta = 90^\circ$

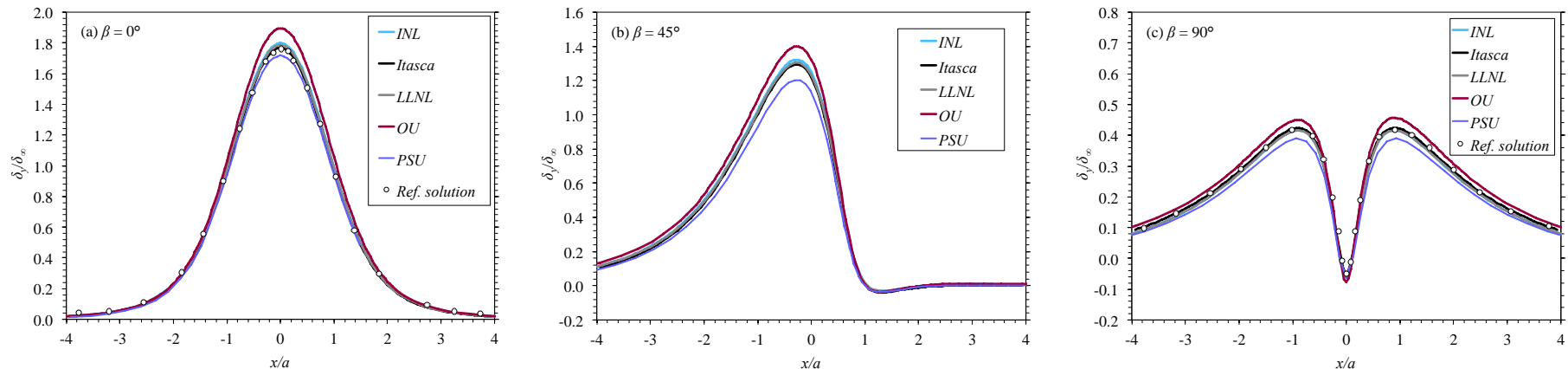


Surface vertical displacement with various dipping angles (reference data by Pollard & Holzhausen (1979))

Case 5. Quantifying Ground Surface Deformation

Participants and Codes Used

Team	Code	Domain	Near-field resolution
Idaho National Laboratory (INL)	FALCON	x: $20a \sim 40a$; y: $11.25a \sim 21.25a$	$0.05a$
Itasca Consulting Group (Itasca)	FLAC3D	x: $25a$; y: $20a$	$0.05a$
Lawrence Livermore National Laboratory (LLNL)	GEOS	x: $40a$; y: $20a$; z: $50a$	$0.05a \sim 0.1a$
University of Oklahoma (OU)	GEOFRAC	x: $50a$; y: $50a$; z: $50a$	$0.04a \sim 0.07a$
Penn State University (PSU)	FLAC3D	x: $40a$; y: $15 \sim 17a$	$0.05a \sim 0.1a$
University of Texas at Austin (UT Austin)	CFRAC_UT	N/A	$0.015a$



Comparison of 2D surface deformation results submitted by five teams (reference data by Pollard & Holzhausen (1979))

Artworks by **P. Fu & B. Guo** at Lawrence Livermore National Laboratory

Case 5. Quantifying Ground Surface Deformation

- Surface deformation predictions made by all the participating teams are very close to each other. This is especially encouraging considering the variety of numerical methods (FEM, FEM, BEM, and bonded particle type method) used.
- The analysis of the results revealed the importance using sufficiently large domain sizes to approximate the infinite domain and using appropriate mesh resolutions.

Acknowledgment

- This work was supported by the U.S. Department of Energy, under a DOE Idaho Operations Office Contract. Accordingly, the U.S. Government retains a nonexclusive, royalty-free license to publish or reproduce the published form of this contribution, or allow others to do so, for U.S. Government purposes.